Communication

A Wideband High-Gain Multi-Linear Polarization Reconfigurable Antenna

Dingzhao Chen, Yanhui Liu, *Senior Member, IEEE*, Shu-Lin Chen, Pei-Yuan Qin, *Member, IEEE*, and Y. Jay Guo, *Fellow, IEEE*

***Abstract*—In this Communication, a wideband low-profile antenna with switchable multi-linear polarizations (MLPs) is proposed. An odd number of dipoles with trapezoidal-shaped arms printed on both sides of a substrate are adopted as reconfigurable radiators, which provides a much smaller polarization interval than using an adjacent even number of dipoles. PIN diodes with simple DC biasing lines are loaded to reconfigure the polarization states. A circular-contoured artificial magnetic conductor (AMC) reflector using hexagon-patch cells is employed to reduce the antenna profile. The whole multiple dipole structure is rotationally invariant which provides almost rotationally invariant antenna performance for different LPs. In addition, the antenna can be easily re-designed when adjusting the number of dipoles for different LPs. A seven-LP reconfigurable antenna working in 2.85 GHz to 3.40 GHz is used as an example to give the detailed parameters study and performance analysis. Three antennas with 5, 7 and 9 reconfigurable LPs are designed and measured. With 0.035λ height, they achieve the measured overlapped bandwidths of 20.6%, 17.6% and 15.9% for 5, 7 and 9 LPs, respectively, and their measured peak gains are ranging from 8.3 to 8.5 dBi.**

***Index Terms*—Multi-linear polarization reconfigurability; reconfigurable antenna; artificial magnetic conductor (AMC).**

I. Introduction

POLARIZATION reconfigurable antennas have received much attention in recent years due to the advantages of reducing polarization mismatching loss [1] and suppressing signal fading loss caused by multi-path effects [2]. In the past, in order to achieve better polarization matching for arbitrarily polarized waves, many polarization-reconfigurable antenna designs have been presented such as in [3]–[9], and most of them focus on the reconfigurability among two orthogonal circular polarizations (CPs) and two orthogonal linear polarizations (LPs). It is well understood that when applied to receive arbitrary LP waves, they may cause as much as 50% power loss.

Thus, to overcome the polarization mismatch problem for an arbitrary LP wave, some recent research has been reported to design multi-linear polarization (MLP) reconfigurable antennas [10]–[20]. Despite the success of them, to the best of our knowledge, obtaining a relatively large number of LPs (e.g., 6 or more LPs with an interpolation interval of 30° or less) while maintaining a relatively wider bandwidth (e.g., more than 15% relative bandwidth) remains a challenging problem due to the following two aspects: a) First, most of the existing MLP antennas with 6 or more LPs have quite narrow relative bandwidths [13]–[17]. For example, in [14], an outer circular-ring patch is connected a center pad and cut into several pieces to achieve 6 reconfigurable LPs. However, due to the basic microstrip patch mode, it suffers from narrow impedance bandwidths which is only 1.5%. In [15], a polarization reconfigurable antenna based on ring slot on circular substrate-integrated waveguide (SIW) is proposed. The 22.5° polarization reconfigurable interval can be achieved by connecting short strips via PIN diodes in different directions on the ring slot. Since the SIW cavity works in the fundamental TE_{10} mode, the antenna's overlapped bandwidth is less than 5.1%; b) Second, although some of MLP antennas have relatively wide bandwidths, the achievable number of LPs are basically no more than 4, and it is hard to considerably increase the number of LPs due to their particular implementation mechanisms [18]–[20]. For example, in [19], a wideband four-LPs reconfigurable antenna is presented in which four pairs of trapezoidal dipoles are printed on the top layer of the substrate and excited by the same feeding source provided by a tapered Balun in vertical plane. This multi-dipole structure is symmetric about the planar Balun, and thus the coupling environment of dipoles for different LPs is different. This difference becomes significantly enhanced with the increase of the number of dipoles, which will result in the significant performance difference among different LP states and thus reduce the overlapped bandwidth. In addition, since all the arms of dipoles are printed on the same side of the substrate, there are no much space to considerably increase the number of shaped dipoles used in the antenna.

In this Communication, a simple yet effective configuration based on rotationally invariant trapezoidal dipoles and reconfigurable feeding structure is developed to achieve a wideband, almost rotationally invariant performance for different LP states. A circular-contoured artificial magnetic conductor (AMC) reflector using hexagon-patch cells is employed to reduce the antenna profile. The proposed design exhibits the following valuable features: a) The radiating dipole arms are separated on both sides of the substrate, which allows us to arrange a more number of trapezoidal dipole arms than the way of putting all the arms on the same side of the substrate; b) An odd number of dipoles are adopted which can generate more number of LPs with less polarization intervals than using even number of dipoles such as in [19], [20], as an even number of dipoles can provide only half of that number of LPs; c) The proposed multi-dipole structure integrated with the reconfigurable feeding network and the AMC is almost rotationally invariant for exciting different LPs, and consequently the antenna performance is basically invariant for different LPs. This property is desired for most of applications, and it also allows us to have an easy design and optimization of the antenna when balancing the performance of exciting different dipoles.

As an illustration, a seven-LP reconfigurable antenna working in 2.85 GHz to 3.40 GHz is designed to give the detailed parameters study and performance analysis. The height is 3.40 mm that is equal to 0.035λ at 3.10 GHz. Measurement results show that the antenna can achieve switchable seven LPs with a polarization interval of only 25.7°, while remaining a 17.6% overlapped bandwidth that is much wider than those obtained with a similar number of LPs in [13]–[17]. The measured peak gain over the working band reaches 8.5 dBi that is relatively higher than most of reconfigurable antennas. In addition, we have also designed and measured the antennas with 5 and 9 reconfigurable dipoles, and the effect of increasing the number

Manuscript received xxx. This work was supported by the National Natural Science Foundation of China (NSFC) under Grant No. 61871338. (Corresponding author: Yanhui Liu).

D. Chen is with the Institute of Electromagnetics and Acoustics, Xiamen University, Fujian 361005, China.

Y. Liu is with the School of Electronic Science and Engineering, University of Electronic Science and Technology of China, Chengdu 611731, China, (e-mail: yhliu@uestc.edu.cn)

S.-L. Chen, P. Y. Qin and Y. Jay Guo are with the Global Big Data Technologies Centre, University of Technology Sydney (UTS), NSW 2007, Australia.

of dipoles on the antenna performance is analyzed.

II. Antenna Design and Analysis

In this section, configuration of the proposed MLP reconfigurable antenna using the seven-LP reconfigurability case as an example is introduced. Subsequently, detailed biasing strategy for the PIN diodes is described, and the performance of AMC employed in this antenna is also discussed. Then, the effect of key parameters on the performance of the seven-LP reconfigurable antenna is analyzed.

A. Antenna Configuration

Configuration of the developed seven-LP reconfigurable antenna is shown in Fig. 1. The antenna is mainly composed of seven pairs of electric dipoles and an AMC reflector. The seven dipoles are arranged in rotational symmetry to realize a 25.7° polarization interval. In order to achieve a wide overlapped bandwidth, trapezoidal-shaped dipoles are utilized. This antenna is designed to work at the central frequency of 3.1 GHz.

The lateral view of the antenna is shown in Fig. 1(a). As can be seen, the antenna consists of two substrates, i.e., substrate 1 and substrate 2. Both of these two substrates are two-layer copper-clad. Between substrate 1 and 2, there is an air gap with a height h. The following are the parameters of substrate 1: relative permittivity $\varepsilon_r = 2.2$, loss tangent $\tan\delta = 0.0009$, thickness = 0.5 mm, and radius $R_1 = 30$ mm. The relative permittivity, loss tangent, thickness and radius (R_2) of substrate 2 are 4.4, 0.02, 2.4 mm, and 65 mm, respectively.

Fig. 1(b) shows the top and bottom views of substrate 1. On the top of substrate 1, a circular feed pad with a radius R_0 is centrally printed, as seen in the left of Fig. 1(b). Seven trapezoidal-shaped patches are uniformly distributed around the central pad, and their dimensions are represented by L and W. The seven patches are labelled as #1 to #7 in a counter-clockwise direction. In this design, PIN diodes are chosen to realize the reconfigurability control between seven LPs. The PIN diodes are placed between the central pad and each of the trapezoidal-shaped patches. The close view of these PIN diodes is shown at the top of Fig. 1(b). The positive polarity of each PIN diode is connected to the central pad, and its negative polarity is attached to the trapezoidal-shaped patch. A small DC pad is printed with a small gap to each of the patches. These gaps are bridged with inductors to block the RF signal while maintaining the DC continuity. On the bottom of substrate 1, as seen in the right of Fig. 1(b), all the central pads, trapezoidal-shaped patches and DC pads are rotated by 180° with regard to the corresponding parts printed on the top.

Fig. 1(c) shows the top view of substrate 2. Thirty seven hexagonal patches are evenly printed. Each hexagon-patch cell has a side length of d, and a small gap with a width of S exists between every two adjacent hexagonal patches. A solid ground plane is placed on the bottom of substrate 2. Note that several air holes are drilled through the substrate 1 and 2 for placing the DC biasing wires.

The dipoles of this antenna are fed by differential mode via the central feed pads on the top and bottom of the substrate 1 that are connected to the inner and outer conductors of a 50 Ω coaxial cable. No Balun is used due to its high profile. The size of the feed pads should be properly chosen by considering good impedance matching and enough space to connect the multiple PIN diodes. Due to the air gap between substrate 1 and 2, an dielectric annular cylinder is used to support the substrate 1. This dielectric has the same permittivity and loss tangent as those of substrate 1. The following are parameter values: $h = 0.5$ mm, $R_0 = 1.5$ mm, $L = 16$ mm, $W = 10$ mm, $d = 10$ mm, $S = 0.4$ mm.

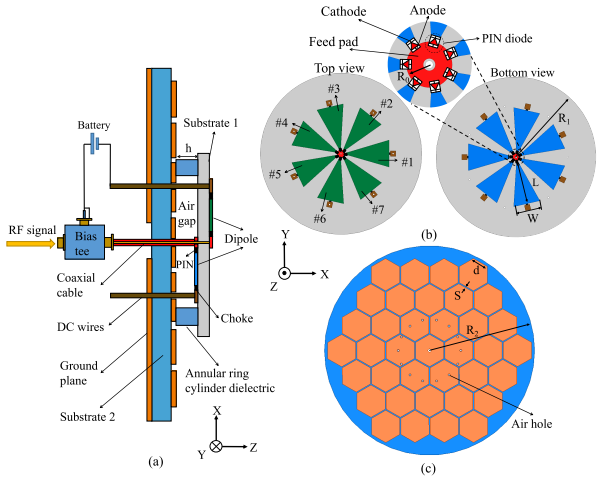

Fig. 1: Geometry of the proposed antenna with switchable seven-LPs. (a) Sectional drawing along x-axis, (b) top view and bottom view of substrate 1, and (c) top view of substrate 2.

B. Operating Mechanism and DC Biasing Strategy

The developed antenna can reconfigure among seven LPs at an interval of 25.7° by switching the PIN diodes. For a particular polarization state, e.g., x-axis polarization, one needs to switch on the pair of PIN diodes loaded on the x-axis, i.e., the two diodes between the top/bottom #1 trapezoidal-shaped patch and the center feed. Thus, only a pair of patches #1 are connected to the central pads, while the other patches are disconnected. In this manner, the two connected patches act as two arms of a dipole antenna, and thus the linear polarization along x-axis is achieved at this working state. Similarly, by controlling the other pairs of the PIN diodes, a total of seven LPs (denoted as state 1 to 7 in Fig. 1) can be reconfigured. As shown in Fig. 1, the antenna configuration at different LP states is rotationally invariant, which benefits the antenna optimization and measurement.

The PIN diodes are Bar50-02L with 0402 surface mount packaging produced by Infineon Company [21]. According to its datasheet, the diode can be equivalent to a 3 Ω resistor in series with a 0.4 nH inductor at its 'ON' state, and a 5000 Ω resistor in parallel with a 0.1 pF capacitor and in series with a 0.4 nH inductor at its 'OFF' state. Through simulating and measuring the performance of a microstrip line loaded with the PIN diode, we have conformed that the PIN diode has nearly linear response when a signal within the working frequency band of the antenna goes through this diode. The inductors (15 nH) are VHF100505H15NJ with 0402 surface mount packaging produced by FH High Technology Company [22]. They can effectively choke the RF signals while maintaining the DC continuity in the frequency band from 2.5 to 4.0 GHz. Simple yet effective DC biasing network is developed to control the states of these diodes. As shown in Fig. 1(a), the battery provides the bias voltage to both ends of PIN diode through the bias tee and the DC wires.

C. Artificial Magnetic Conductor (AMC) Using Hexagonal Patches

As is well known, a dipole antenna has omnidirectional radiation in its H-plane. In order to enhance the radiation directivity, a PEC reflector can be usually placed behind the dipole to block the backward radiation. However, the PEC reflector typically leads to a high-profile of $\lambda_0/4$. Thus, replacing the PEC with an AMC would be a good way to realize a low-profile antenna as the AMC can provide a near 0° reflection phase [23], [24]. For single and dual polarized antennas,

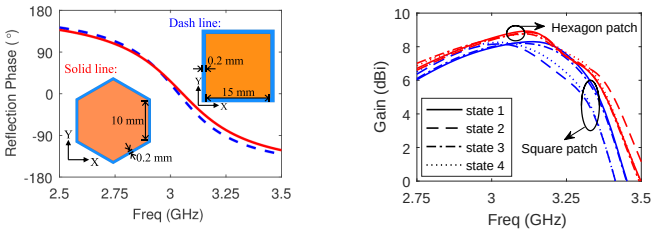

(a) (b)

Fig. 2: The performance comparison of the seven-LP antennas with hexagonal and squared patch AMC reflectors. (a) The simulated reflection phases of two units, and (b) the simulated antenna gains.

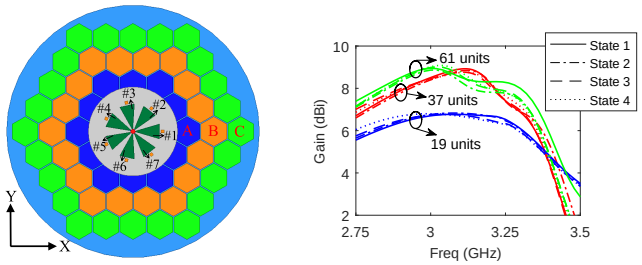

(a) (b)

Fig. 3: (a) The geometry of the seven-LP antennas using three sizes of AMCs with 19, 37 and 61 units (their outermost ring of units are denoted by A, B and C, respectively), and (b) their simulated gains.

AMC reflectors are usually made of squared patches. However, for the developed reconfigurable antenna with seven LPs, a square-bounded AMC reflector may result in performance variation among different polarization states of the antenna. Here we choose hexagonal patches as the unit cells such that a nearly circular-contoured AMC can be formed to provide more uniform performance for different LPs. As an illustration, Fig. 2(a) shows the phase responses of the designed squared and hexagonal patch cells that are obtained by simulation in High Frequency Structure Simulator (HFSS) with periodic boundary conditions, and Fig. 2(b) shows the simulated radiation gain values versus the frequency of the seven-LP antennas integrated with 1) the square-bounded AMC composed of 7×7 squared patches and 2) the proposed circular-contoured AMC composed of 37 hexagonal patches. Note that except for the AMC difference, all the parameters for the two antennas are the same. Besides, the antenna configurations at state 5, 6 and 7 is completely symmetrical about x-axis with the configurations at state 4, 3 and 2, respectively, as shown in Fig.1. Thus, the simulated gain values only at the first four LP states are shown here. As can be seen, both of the squared and hexagonal cells have the reflection phases within $\pm 90^\circ$ within the band from 2.85 to 3.35 GHz. However, the antenna with the circular-contoured hexagonal patch AMC can provide much more uniform performance for different LPs than the antenna using the squared patch AMC.

On the other hand, to determine an appropriate number of hexagonal patch cells used in the AMC, we simulate the antennas with three sizes of AMC reflectors that have 19, 37 and 61 hexagonal patches. Their geometries are briefly shown in Fig. 3(a). Fig. 3(b) shows the simulated gain values versus frequency for the three antennas with different sizes of AMCs. As can be seen, when the number of units increases from 19 to 37, the maximum gain value is improved from 6.7 to 9.0 dBi. With a further increase of the number to 61, the maximum gain value keeps similar. Hence, the AMC with 37 hexagonal patch cells is adopted for the proposed antenna.

D. Parameters Study

For the proposed antenna structure, there are three essential parameters influence the antenna performance, the length L and width W of the trapezoidal-shaped dipole arm and the radius R_0 of the top and bottom feed pads. L and W have significant impacts on the impedance matching and bandwidth, and R_0 influences the transition impedance from the coaxial cable to dipoles. For simplicity, we take the dipole pair #1 of the antenna (denoted by state 1) as an example to study the effects of these parameters. The obtained results are similar as those by turning on any one of other dipole pairs of the proposed antenna due to the almost rotationally invariant antenna structure.

At first, consider the effect of the dipole arm length L on the performance of the proposed antenna. Generally speaking, the length L of a thin dipole would be equal to a quarter of the equivalent wavelength λ_e which can be roughly calculated as $\lambda_0/\sqrt{(\varepsilon_r+1)/2}$. However, the adopted dipole has a trapezoidal-shaped arm, which usually shorten the required length. Thus, we obtain that $L \leq \lambda_0/\sqrt{8(\varepsilon_r+1)}$. For the case of $\varepsilon_r = 2.2$ and $f_0 = 3.1$ GHz, we can roughly estimate $L \leq 19.1$ mm. Here, we set $L = [14, 16, 18]$ mm with a fixed $W = 10$ mm and $R_0 = 1.5$ mm to test the effect of using different L. Fig. 4(a) shows the simulated $|S_{11}|$ of the antenna within the band from 2.75 to 3.5 GHz, and Fig. 4(b) shows co- and cross-polarization radiation gains of the antenna. As can be seen, the antenna with either $L = 16$ mm or 18 mm achieves relatively better impedance matching performance than the one with $L = 14$ mm. Compared with the case of $L = 18$ mm, using $L = 16$ mm gives a stably low cross-polarization level across the interested band.

For the trapezoidal-shaped dipole, increasing the width W usually leads to less frequency-dependency of impedance and wider bandwidth. On the other hand, the Q of antenna is inversely proportional to its bandwidth. The smaller the Q value, the flatter the gain curve of the antenna. This means that as the antenna bandwidth increases, the peak gain probably decreases. Meanwhile, the antenna performance is also influenced by the coupling between neighboring dipole arms. Thus, the value of W is not necessarily the larger the better. In Fig. 5, the results for different W are displayed. Evidently, when W changes, the impedance matching changes considerably. As shown in Fig. 5(b), the gain versus frequency becomes flatter when W is increased from 8 mm to 12 mm. Using $W = 10$ mm gives the best total performance in terms of both impedance matching and the realized gain over the interested band.

The feed pads are connected to the coaxial line and the dipoles. Its size determined by R_0 has a significant effect on the impedance of the antenna. Fig. 6(a) and (b) show the the effect of R_0 on the antenna input reflection coefficient and gain, respectively. Obviously, when $R_0 = 2.2$ mm, the $|S_{11}|$ of this antenna is not satisfactory. When $R_0 = 0.8$ mm or 1.5 mm, the antenna can obtain a relatively larger bandwidth. The realized gain is not greatly influenced by the variation of R_0. Taking into account the size of PIN diode and the difficulty of welding, a relatively larger $R_0 = 1.5$ mm is suggested.

III. Simulated and Measured Results

We have fabricated a prototype of the developed reconfigurable seven-LP antenna with its parameters given in Section II-A, as shown in Fig. 7. Its performance is measured using a far-field antenna measurement system in microwave chamber, located at Haiyun campus, Xiamen University. As mentioned previously, due to the symmetry of the antenna structure about x-axis, the antenna performances at state 2 to 4 are the same as those at state 7 to 5, respectively. So only the first four states (i.e., state 1 to 4) are demonstrated for simplicity. Fig. 8(a) shows the simulated and measured $|S_{11}|$s for state 1 and 2, and Fig. 8(b) shows the simulated and measured $|S_{11}|$s for state

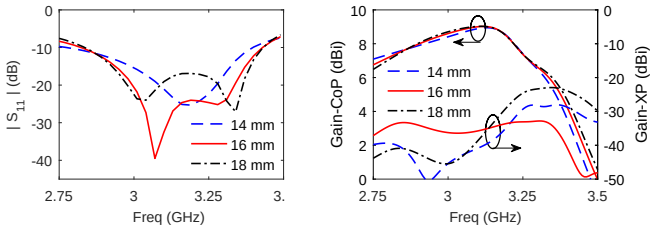

(a) (b)

Fig. 4: The effect of varying L on the performance of the seven-LP reconfigurable antenna at state 1. (a) $|S_{11}|$, and (b) co- and cross-polarization gains versus frequency.

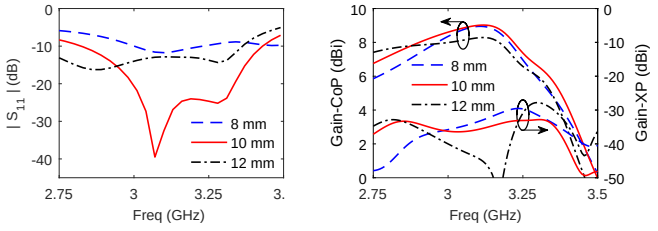

(a) (b)

Fig. 5: The effect of varying W on the performance of the seven-LP reconfigurable antenna at state 1. (a) $|S_{11}|$, and (b) co- and cross-polarization gains versus frequency.

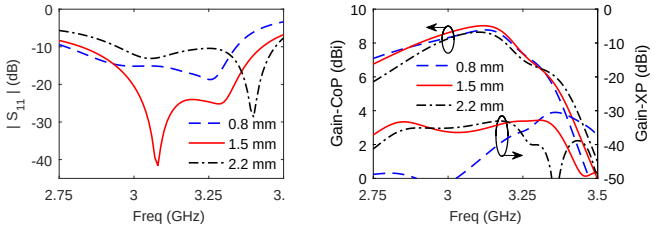

(a) (b)

Fig. 6: The effect of varying R_0 on the performance of the seven-LP reconfigurable antenna at state 1. (a) $|S_{11}|$, and (b) co- and cross-polarization gains versus frequency.

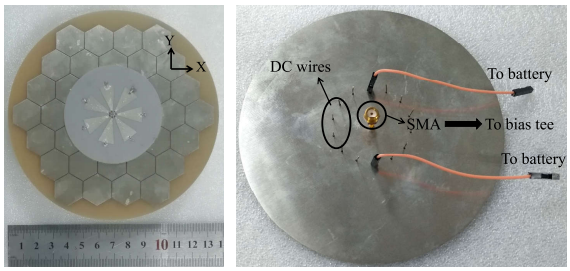

Fig. 7: Photos of the fabricated seven-LP reconfigurable antenna.

3 and 4. The simulated overlapped impedance bandwidth in terms of $|S_{11}| \leqslant -10$ dB for all the four states is from 2.82 GHz to 3.40 GHz, while the measured overlapped bandwidth is from 2.85 GHz to 3.40 GHz. Although there exists some differences between the measured and simulated $|S_{11}|$s due to possible fabrication errors, their bandwidths for $|S_{11}| \leqslant -10$ dB are almost the same for each state. Consequently, the measured overlapped bandwidth agrees well with the simulated one. The measured relative overlapped bandwidth of this antenna reaches 17.6% which is relatively wide for a seven-LP antenna.

Fig. 9(a) shows the variations of simulated and measured radiation

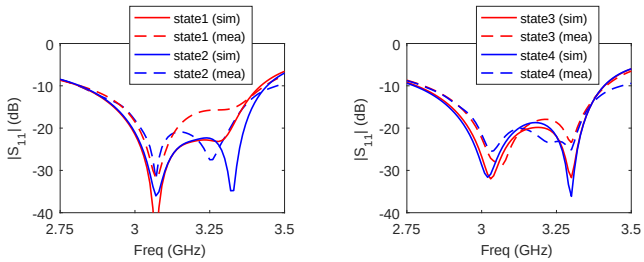

(a) (b)

Fig. 8: The simulated and measured $|S_{11}|$s of the seven-LP reconfigurable antenna. (a) State 1 and 2, and (b) state 3 and 4.

gains versus frequency of the proposed antenna at state 1 to 4, and Fig. 9(b) show the simulated and measured radiation efficiency. For checking the effect of PIN diodes on the gain and efficiency, we simulated the antenna with two different PIN diode models: 1) model A is the equivalent circuit model of the PIN diode as described in Section II-B (it is also adopted in all of other simulations in this paper), and 2) model B is an ideal model that simply considers the 'ON' and 'OFF' states of the diode as 'connection' and 'disconnection' of a PEC line. As can be seen, the gain curves for all the four states are very similar to each other in terms of all the simulated (for both model A and B) and measured results. Compared with the ideal model B, the antenna using the more realistic PIN model A has a degradation of 0.5 to 1 dB in gain in the band from 2.85-3.40 GHz, and accordingly the simulated efficiency using model A is also reduced by about 9% on the average in this band. The measured results are close to the simulated ones with model A with a small additional degradation in both gain and efficiency mainly due to the insert loss of bias tee and the influence of RF chokes. Nevertheless, the measured peak gain reaches about 8.5 dBi for each polarization state, which is still high for a single antenna. The measured efficiency is ranging from 65.14% to 74.44% in the band of 2.85-3.40 GHz. Besides, the measured cross-polar. gains are about 20 to 25 dB lower than the corresponding co-polar. gains within the whole overlapped bandwidth for all polarization states of this antenna.

Fig. 10(a)-(d) show the radiation patterns at 3.1 GHz in both E- and H-planes for state 1 to 4 of the seven-LP reconfigurable antenna, respectively. The E-planes for state 1 to 4 are the planes with $\varphi = [0°, 51.4°, 102.9°, 154.3°]$, respectively, and the H-planes are orthogonal to the corresponding E-planes. As can be seen, the co-polarization patterns in both E- and H-planes for different states are very similar. This means that the radiation pattern is almost rotationally invariant for different states of the antenna. This property also holds at other frequency in the working frequency band. In the maximum radiation direction, the cross-polarization level is more than 20 dB lower than the co-polarization level for all states. Such a polarization isolation is usually acceptable for most applications.

IV. Discussion and Comparisons

A. Discussion on Arrangement of Reconfigurable Dipoles

In addition to achieving the seven-LP reconfigurability, the proposed antenna can also obtain other number of reconfigurable LPs by changing its number of dipoles. The discussion on the multiple dipole arrangement in terms of achievable number of LP states and the corresponding bandwidths is necessary. As shown in Fig. 1, two arms of each dipole in the proposed antenna structure are printed on top and bottom of the substrate 1, respectively. It is easily observed that if an even number of dipoles is adopted, for each dipole among them, we can always find another dipole oriented inversely to this

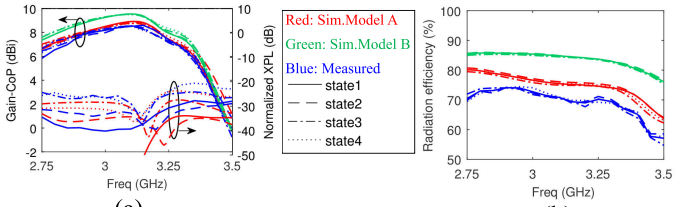

(a) (b)

Fig. 9: (a) The simulated and measured gains and cross-polar. levels versus frequency for state 1 to 4 of the seven-LP antenna, and (b) the simulated and measured radiation efficiency. Two different models are used for the PIN diodes for comparison.

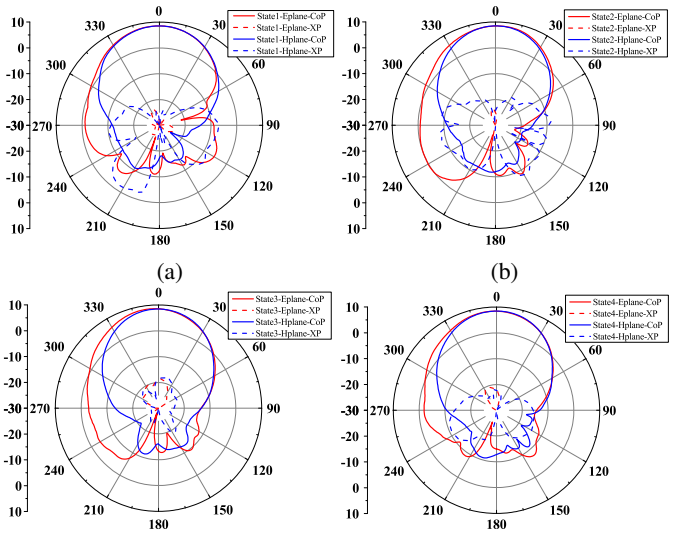

(a) (b) (c) (d)

Fig. 10: The measured co- and cross-polar. patterns in E- and H-planes at 3.1 GHz for the reconfigurable antenna at (a) state 1, (b) state 2, (c) state 3, and (d) state 4.

dipole. This means that the achievable polarization number is only half of the number of dipoles used. This does not happen when the number of dipoles is odd. For example, Fig. 11(a) and (b) show the geometries of two antennas with different dipole arrangements: one has fourteen reconfigurable dipoles and the other has seven dipoles. As can be seen, although they have different numbers of dipoles, they actually achieved the same seven-LP reconfigurability with the same polarization interval of 25.7°. Compared with the case of using fourteen reconfigurable dipoles, the antenna with seven dipoles have a larger angular space for each trapezoidal-shaped arm which in general leads to a larger bandwidth achieved. To verify this, we simulate the antennas with these two different dipole arrangements. Their parameters including the dipole arm lengths (L) and widths (W) are optimized as provided in Table I. Fig. 12(a) and (b) show the simulated $|S_{11}|$s of the two antennas with seven and fourteen dipoles, respectively. Due to the symmetry along x-axis, the results are shown only for the first four states of the antenna. It is observed that the simulated overlapped bandwidth for the reconfigurable antenna with seven dipoles is 18.6%, while it is only 13.9% for the antenna with fourteen dipoles.

Besides, increasing the number of dipoles results in the reduction of polarization interval, so that the maximum polarization mismatch for receiving an arbitrarily linearly polarized wave can be reduced. As is known, the polarization mismatch is given by $\eta_{\text{pol}} = 20\log_{10}(\vec{p}_r \cdot \vec{p}_{\text{inc}})$, where $\vec{p}_r$ and $\vec{p}_{\text{inc}}$ are the polarization direction vectors of the receiving antenna and incident wave, respectively. For the proposed MLP antennas with N reconfigurable

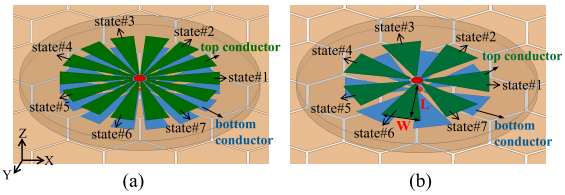

(a) (b)

Fig. 11: Top views of two different seven-LP reconfigurable antennas with (a) fourteen and (b) seven dipoles.

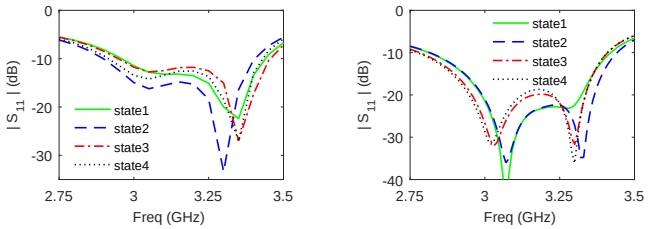

(a) (b)

Fig. 12: The simulated $|S_{11}|$ characteristics of two different seven-LP antennas with (a) fourteen and (b) seven dipoles, respectively.

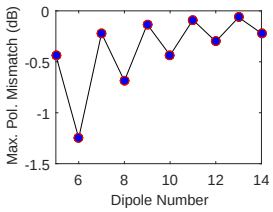

Fig. 13: The maximum polarization mismatch loss versus the number of dipoles employed in the reconfigurable antenna.

TABLE I: THE OPTIMIZED DIPOLE DIMENSIONS FOR THE RECONFIGURABLE ANTENNAS WITH DIFFERENT NUMBERS OF DIPOLES.

Dipole Num.		Five	Seven	Nine	Fourteen
Dipole Dimensions	Length (L)	16 mm	16 mm	16 mm	18 mm
	Width (W)	12 mm	10 mm	7 mm	6 mm

dipoles, the maximum polarization mismatch can be calculated by $\eta_{\max} = 20\log_{10}(\cos[\pi/(N+(1-(-1)^N)N/2)])$. This relationship is depicted in Fig. 13. As can be seen, using an odd number of dipoles have much less polarization loss than using its adjacent even number of dipoles. The antennas with 7 and 9 dipoles give the maximum polarization mismatch of -0.22 and -0.13 dB, respectively, and further increasing the dipole number would not be necessary.

To study the effect of increasing the dipole number on the achievable bandwidth of the proposed antenna, we have designed, fabricated and measured two additional antennas with five and nine reconfigurable dipoles, respectively. The photographs of them are shown in Fig. 14. Their dipole arm lengths and widths are optimized as provided in Table I. Fig. 15(a) and (b) show the simulated and measured $|S_{11}|$s for the reconfigurable antennas with five and nine dipoles, respectively. As can be seen, the simulated and measured overlapped bandwidths for the antenna with five dipoles are 21.1% and 20.6%, respectively, and they are 17.8% and 15.9% for the antenna with nine dipoles. It is mentioned that the simulated and measured bandwidths is 18.6% and 17.6% for the case of seven dipoles. Thus, it is confirmed that the achievable bandwidth decreases as the number of dipoles used increases mainly due to the reduced width of the trapezoidal-shaped arms.

B. Comparative Study on Antenna Performance

Table II lists the statistical data of the proposed MLP reconfigurable antennas with five, seven and nine dipoles as well as other MLP-

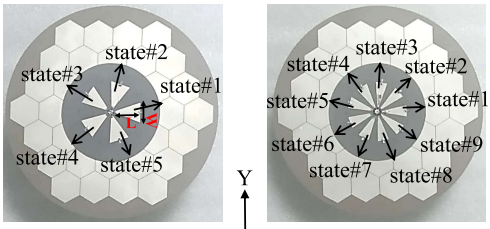

Fig. 14: Photographs of the fabricated two reconfigurable antennas with (a) five dipoles and (b) nine dipoles.

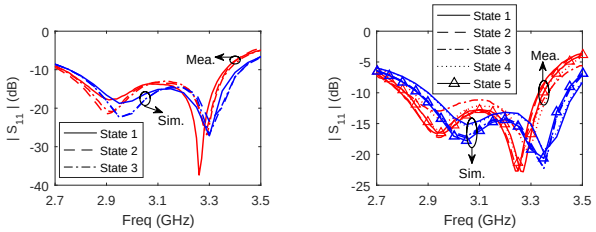

Fig. 15: The simulated and measured $|S_{11}|$s of the proposed reconfigurable antennas with (a) five dipoles and (b) nine dipoles.

TABLE II: PERFORMANCE COMPARISON WITH REPORTED MULTI-LINEAR POLARIZATION RECONFIGURABLE ANTENNAS

Ref.	No. of LPs	Polarization interval (°)	Overlapped BW	Peak gain (dBi)	Aperture size (λ^2)	Profile height (λ)
[11]	4	45	2.5%	6.9	0.44	0.024
[12]	4	45	7.0%	5.9	0.32	0.07
[18]	4	45	17.6%	6.1	0.35	0.08
[19]	4	45	34.0%	5.2	0.61	0.26
[20]	4	45	53.9%	10.9	1.59	0.13
[14]	6	30	1.5%	3.52	1.08	0.03
[16]	8	22.5	2.50%	6	1.29	0.08
This work	5	36	21.1% (Sim.)	8.5 (Sim.)	1.41	0.035
			20.6% (Mea.)	8.3 (Mea.)		
	7	25.7	18.6% (Sim.)	9.0 (Sim.)	1.41	0.035
			17.6% (Mea.)	8.5 (Mea.)		
	9	20	17.8% (Sim.)	8.7 (Sim.)	1.41	0.035
			15.9% (Mea.)	8.4 (Mea.)		

reconfigurable antennas in literatures. All these antennas have the reconfigurability among four or more LPs. The electrical sizes of these antennas are calculated at their respective center operating frequencies. Compared with the works in [11], [12], [18]–[20], the proposed MLP antennas have more number of LPs with smaller polarization intervals which leads to a significantly reduced loss in the maximum polarization mismatch. Compared with the six- and eight-LP reconfigurable antennas in [14] and [16], the proposed antennas achieve much wider bandwidth performance. The obtained peak gains for the proposed antennas are also relatively higher than those for most of the reported MLP-reconfigurable antennas.

V. CONCLUSION

In this communication, a multi-linear polarization (MLP) reconfigurable antenna by symmetrically arranging multiple trapezoidal-shaped dipoles integrated with an AMC reflector is developed. Parameters study is given in detail for a seven-LP reconfigurable antenna. Since the whole multiple dipole structure is rotationally invariant, which benefits the antenna's design and applications. Three antennas with five, seven and nine reconfigurable dipoles have been designed and measured. The measurement results are in good agreement with simulated ones, which validates the effectiveness of the proposed designs. Compared with the four-LP reconfigurable antennas in literatures, the proposed antennas with switchable five, seven and nine-LPs have relatively smaller polarization intervals with reduced polarization mismatch loss. Compared with the reported six and eight-LP antennas, the proposed antennas have much better bandwidth performance.

REFERENCES

[1] J. T. Bernhard, R. Wang, R. Clark, and P. Mayes, "Stacked reconfigurable antenna elements for space-based radar applications," *IEEE Antennas Propagat. Int. Symp.*, Boston, MA, USA, 2001, vol. 1, pp. 158-161.

[2] C. G. Christodoulou, Y. Tawk, S. A. Lane, and S. R. Erwin, "Reconfigurable antennas for wireless and space applications," *Proc. IEEE*, vol. 100, no. 7, pp. 2250-2261, Jul. 2012.

[3] S. Gao, A. Sambell, and S. S. Zhong, "Polarization-agile antennas," *IEEE Antennas Propag. Mag.*, vol. 48, no. 3, pp. 28-37, Jun. 2006.

[4] D. Rodrigo, B. A. Cetiner, and L. Jofre, "Frequency, radiation pattern and polarization reconfigurable antenna using a parasitic pixel layer," *IEEE Trans. Antennas Propag.*, vol. 62, no. 6, pp. 3422-3427, Jun. 2014.

[5] L. Ge, X. Yang, D. Zhang, M. Li, and H. Wong, "Polarization-reconfigurable magnetoelectric dipole antenna for 5G Wi-Fi," *IEEE Antennas Wireless Propag. Lett.*, vol. 16, pp. 1504-1507, 2017.

[6] J.-S. Row and M.-J. Hou, "Design of polarization diversity patch antenna based on a compact reconfigurable feeding network," *IEEE Trans. Antennas Propag.*, vol. 62, no. 10, pp. 5349-5352, Oct. 2014.

[7] J. Hu, Z.-C. Hao, and W. Hong, "Design of a wideband quad-polarization reconfigurable patch antenna array using a stacked structure," *IEEE Trans. Antennas Propag.*, vol. 65, no. 6, pp. 3014-3023, Jun. 2017.

[8] F. Wu and K. M. Luk, "A reconfigurable magneto-electric dipole antenna using bent cross-dipole feed for polarization diversity," *IEEE Antennas Wireless Propag. Lett.*, vol. 16, pp. 412-415, 2017.

[9] W. Li, X. Tang and Y. Yang, "Design and implementation of SIW cavity-backed dual-polarization antenna array with dual high-order modes," *IEEE Trans. Antennas Propag.*, vol. 67, no. 7, pp. 4889-4894, Jul. 2019.

[10] J. S. Row and Y-J. Huang, "Reconfigurable antenna with switchable broadside and conical beams and switchable linear polarized patterns," *IEEE Trans. Antennas Propag.*, vol. 66, no. 7, pp. 3752-3756, Jul. 2018.

[11] H. Gu, J. Wang, L. Ge, and C.-Y.-D. Sim, "A new quadri-polarization reconfigurable circular patch antenna," *IEEE Access*, vol. 4, pp. 4646-4651, 2016.

[12] S.-L. Chen, F. Wei, P.-Y. Qin, Y. J. Guo, and X. Chen, "A multi-linear polarization reconfigurable unidirectional patch antenna," *IEEE Trans. Antennas Propag.*, vol. 65, no. 8, pp. 4299-4304, Aug. 2017.

[13] N. Nguyen-Trong, A. Piotrowski, L. Hall, and C. Fumeaux, "A frequency- and polarization-reconfigurable circular cavity antenna," *IEEE Antennas Wireless Propag. Lett.*, vol. 16, pp. 999-1002, 2017.

[14] L.-H. Chang, W.-C. Lai, J.-C. Cheng, and C.-W. Hsue, "A symmetrical reconfigurable multipolarization circular patch antenna," *IEEE Antennas Wireless Propag. Lett.*, vol. 13, pp. 87-90, 2014.

[15] P. Vasina and J. Lacik, "Polarization reconfigurable SIW circular ring-slot antenna," *Loughborough Antennas and Propagation Conf. (LAPC)*, Loughborough, UK, 2016, pp. 1-5.

[16] Y. Yang, R. B. V. B. Simorangkir, X. Zhu, K. Esselle, and Q. Xue, "A novel boresight and conical pattern reconfigurable antenna with the diversity of 360° polarization scanning," *IEEE Trans. Antennas Propag.*, vol. 65, no. 11, pp. 5747-5756, Nov. 2017.

[17] C. Xu, Y. Wang, J. Wu, and Z. Wang, "Parasitic circular patch antenna with continuously tunable linear polarization using liquid metal alloy," *Microw. Opt. Techn. Lett.* vol. 61, pp. 727-733, Dec. 2018.

[18] W. Lin and H. Wong, "Multipolarization-reconfigurable circular patch antenna with L-shaped probes," *IEEE Antennas Wireless Propag. Lett.*, vol. 16, pp. 1549-1552, 2017.

[19] H. Wong, W. Lin, L. Huitema, and E. Arnaud, "Multi-polarization reconfigurable antenna for wireless biomedical system," *IEEE Trans. Biomed. Circuits Syst.*, vol. 11, no. 3, pp. 652-660, June 2017.

[20] H. H. Tran, N. Nguyen-Trong, T. T. Le, A. M. Abbosh, and H. C. Park, "Low-profile wideband high-gain reconfigurable antenna with quad-polarization diversity," *IEEE Trans. Antennas Propag.*, vol. 66, no. 7, pp. 3741-3746, Jul. 2018.

[21] Data Sheet of Bar50-02L PIN Diodes, Infineon Technologies, Application Note [Online]. Available: http://www.infineon.com/

[22] Data Sheet of VHF100505H15NJ Inductance, FH High Technologies, Application Note [Online]. Available: http://www.ic37.com/

[23] W. Yang, W. Che, H. Jin, W. Feng, and Q. Xue, "A polarization-reconfigurable dipole antenna using polarization rotation AMC structure," *IEEE Trans. Antennas Propag.*, vol. 63, no. 12, pp. 5305-5315, Dec. 2015.

[24] H. L. Zhu, S. W. Cheung, X. H. Liu, and T. I. Yuk, "Design of polarization reconfigurable antenna using metasurface," *IEEE Trans. Antennas Propag.*, vol. 62, no. 6, pp. 2891-2898, Jun. 2014.